

# Minimizing State-of-Health Degradation in Hybrid Electrical Energy Storage Systems with Arbitrary Source and Load Profiles

Yanzhi Wang<sup>†</sup>, Xue Lin<sup>†</sup>, Qing Xie<sup>†</sup>, Naehyuck Chang<sup>‡</sup>, and Massoud Pedram<sup>†</sup>

<sup>†</sup>University of Southern California, CA, USA, <sup>‡</sup>Seoul National University, Korea

<sup>†</sup>{yanzhiwa, xuelin, xqing, pedram}@usc.edu, <sup>‡</sup>naehyuck@elpl.snu.ac.kr

**Abstract**—Hybrid electrical energy storage (HEES) systems consisting of heterogeneous electrical energy storage (EES) elements are proposed to exploit the strengths of different EES elements and hide their weaknesses. The cycle life of the EES elements is one of the most important metrics. The cycle life is directly related to the state-of-health (SoH), which is defined as the ratio of full charge capacity of an aged EES element to its designed (or nominal) capacity. The SoH degradation models of battery in the previous literature can only be applied to charging/discharging cycles with the same state-of-charge (SoC) swing. To address this shortcoming, this paper derives a novel SoH degradation model of battery for charging/discharging cycles with arbitrary patterns. Based on the proposed model, this paper presents a near-optimal charge management policy focusing on extending the cycle life of battery elements in the HEES systems while simultaneously improving the overall cycle efficiency.

## I. INTRODUCTION

Electrical energy storage (EES) systems are deployed to increase power availability, reliability and efficiency, mitigate the supply-demand mismatch, and regulate the peak-power demand [1]. Unfortunately, none of the existing EES elements, such as Li-ion batteries, lead-acid batteries, and supercapacitors, can simultaneously fulfill all the desirable performance metrics, e.g., long cycle life, high power and energy densities, low cost/weight per unit capacity, high cycle efficiency, and low environmental effects. Hybrid EES (HEES) systems consisting of heterogeneous EES elements are proposed to exploit the strengths of different EES elements and hide their weaknesses for achieving a combination of superior performance metrics [2][3]. It is essential to efficiently implement three management operations: charge allocation, charge replacement, and charge migration [4][5].

Among all the performance metrics, the cycle life of the EES elements is one of the most important metrics that should be considered carefully. The cycle life is directly related to the state-of-health (SoH), which is defined as the ratio of full charge capacity of an aged EES element to its designed (or nominal) capacity. This metric captures the "health" condition of the EES elements, i.e., their ability to store and deliver energy compared to a fresh new one. The SoH degradation models of battery in the previous literature can only be applied to charging/discharging cycles with same state-of-charge (SoC) swing [6][7]. To address this shortcoming, we derive a novel SoH degradation model of battery for charging/discharging cycles with arbitrary patterns. The proposed model is based on an important observation: both a higher SoC swing and a higher average SoC in the charging/discharging cycles will result in a higher SoH degradation rate.

The cycle life of the EES elements in a HEES system is largely dependent on the HEES charge management policy. A recent work [8] proposes an SoH-aware charge management policy for the HEES systems based on the SoH degradation model introduced in [6]. It uses the supercapacitor bank as a buffer to shave the spiky portion of the source or load profiles. This charge management policy has the following limitations: (i) it can only be applied to a two-bank HEES architecture, (ii) it is only effective for source or load profiles in peri-

odic patterns due to the limitation of the SoH degradation model from [6], and (iii) it is based on a simple filter and is far from optimal.

In this work, based on our novel SoH degradation model, we derive a near-optimal charge management policy focusing on extending the cycle life of battery elements in the HEES systems while simultaneously improving the overall cycle efficiency. The SoH-aware charge management policy has the following extensions over [8]:

- It is applicable to the general HEES architecture consisting of multiple battery banks and multiple supercapacitor banks.
- It can be applied for source and load profiles with arbitrary patterns and is no longer limited to profiles in periodic patterns.
- It achieves higher performance, because the optimization of charging/discharging currents depends not only on frequency components but also on magnitudes of source and load profiles.

## II. SOH DEGRADATION MODEL

First, we formally define the SoC and SoH degradation of an EES array. The SoC of an EES array is defined by

$$SoC = C_{array}/C_{full} \times 100\% \quad (1)$$

where  $C_{array}$  is the amount of charge stored in the EES array, and  $C_{full}$  is the amount of charge in the EES array when it is fully charged. We interpret  $SoC$  as the state of the EES array. The  $C_{full}$  value gradually decreases during battery aging (i.e., SoH degradation.) The amount of SoH degradation, denoted by  $D_{SoH}$ , is defined as follows:

$$D_{SoH} = (C_{full}^{nom} - C_{full})/C_{full}^{nom} \times 100\% \quad (2)$$

where  $C_{full}^{nom}$  is nominal value of  $C_{full}$  for a fresh new EES array.

The SoH degradation model in [6] estimates the SoH degradation of a Li-ion battery for cycled charging/discharging, where a (charging/discharging) cycle is defined as a charging process of the battery cell from  $SoC_{low}$  to  $SoC_{high}$  and a discharging process following it from  $SoC_{high}$  to  $SoC_{low}$ . The SoH degradation during one cycle depends on the average SoC level  $SoC_{avg}$  and the SoC swing  $SoC_{swing}$ . We calculate  $SoC_{avg}$  and  $SoC_{swing}$  in one cycle as:

$$SoC_{avg} = (SoC_{low} + SoC_{high})/2 \quad (3)$$

$$SoC_{swing} = SoC_{high} - SoC_{low} \quad (4)$$

$SoC_{swing}$  reaches the maximum value of 1.0 (100%) in a full (100% depth) cycle, i.e., the SoC changes from 0 to 100% and then back to 0. Please refer to the calculation of  $D_{SoH,cycle}(SoC_{swing}, SoC_{avg})$  in [6].

We derive a novel SoH degradation model, which can be applied to charging/discharging cycles with arbitrary patterns. The proposed model extends and generalizes the SoH degradation model introduced in [6] based on the following two observations:

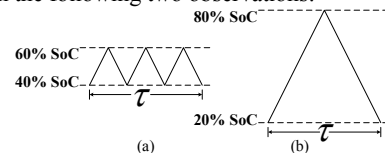


Figure 1: Illustrative example of Observation I.

**Observation I:** The SoH degradation rate is a superlinear function of the SoC swing  $SoC_{swing}$  and the average SoC level  $SoC_{avg}$  [6]. Moreover, the SoC swing has dominant effect over average SoC level.

This work is supported in part by the Software and Hardware Foundations program of the NSF's Directorate for Computer & Information Science & Engineering (No. 1219235) and the Mid-Career Researcher Program and the International Research & Development Program of the NRF of Korea funded by the MSIP (No. 2013075022 and 2013035079). The SPORT lab at USC and ICT at SNU provide research facilities for this study.

An illustrative example of Observation I is provided in Figure 1, which shows two SoC profiles of a battery within the same time duration of  $\tau$ . In Figure 1(a) there are three cycles each with a SoC swing of 20% and an average SoC of 50%, while in Figure 1(b) there is one cycle with a SoC swing of 60% and an average SoC of 50%. The SoC profile in Figure 1(b) results in a higher SoH degradation (about 71.6% higher) though it has a smaller number of charging/discharging cycles.

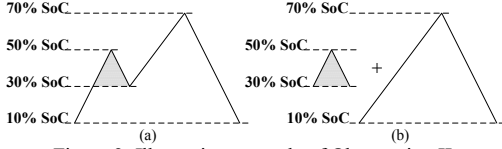


Figure 2: Illustrative example of Observation II.

**Observation II (Decoupling of Cycles):** Consider the SoC profile of a battery cell in Figure 2(a). Although it is not possible to directly apply the model in [6] to estimate SoH degradation, we can perceive it as a combination of two charging/discharging cycles as shown in Figure 2(b). Figure 2(a) and 2(b) are equivalent in terms of the SoC swing and the average SoC, which are the two critical factors.

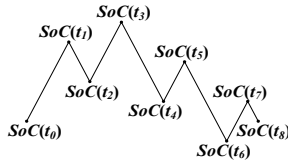


Figure 3: An example battery SoC profile versus time and turning points.

Based on the two observations, we provide the general SoH degradation model as follows. Consider a period  $[0, \tau]$  of charge management. We assume that the duration of the period is too small compared with the battery lifetime (300 – 500 cycles for lead-acid battery or 1500 – 2500 cycles for Li-ion battery [2]) to make any noticeable change in the  $C_{full}$ . Let  $D_{SoH,period}$  denote the total SoH degradation of the Li-ion battery over this period. In the first step, we initialize the value of  $D_{SoH,period}$  to zero. We identify a set of *turning points*  $t_1, t_2, \dots, t_n$ , at which points the battery changes from charging to discharging or from discharging to charging. Figure 3 shows an example SoC profile versus time of a battery and the set of turning points.

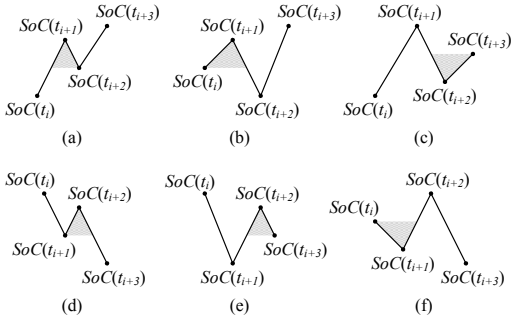


Figure 4: Six basic cases for (charging/discharging) cycle identification.

We identify four consecutive turning points  $(t_i, t_{i+1}, t_{i+2}, t_{i+3})$  from the set of turning points, satisfying one of the following six cases:

- (a)  $SoC(t_i) \leq SoC(t_{i+2}) < SoC(t_{i+1}) \leq SoC(t_{i+3})$ ,
- (b)  $SoC(t_{i+2}) < SoC(t_i) < SoC(t_{i+1}) \leq SoC(t_{i+3})$ ,
- (c)  $SoC(t_i) \leq SoC(t_{i+2}) < SoC(t_{i+3}) < SoC(t_{i+1})$ ,
- (d)  $SoC(t_{i+3}) \leq SoC(t_{i+1}) < SoC(t_{i+2}) \leq SoC(t_i)$ ,
- (e)  $SoC(t_{i+1}) < SoC(t_{i+3}) < SoC(t_{i+2}) \leq SoC(t_i)$ ,
- (f)  $SoC(t_{i+3}) \leq SoC(t_{i+1}) < SoC(t_i) < SoC(t_{i+2})$ .

The six cases are shown in Figure 4(a) - (f). In each case, we identify a complete charging/discharging cycle as shown by the shadowed area in Figure 4(a) - (f). We take case (a) as an example. The SoC swing and average SoC of the identified charging/discharging cycle are:

$$SoC_{swing} = SoC(t_{i+1}) - SoC(t_{i+2}) \quad (5)$$

$$SoC_{avg} = SoC(t_{i+1}) + SoC(t_{i+2})/2 \quad (6)$$

Then we estimate the SoH degradation in this cycle by  $D_{SoH,cycle}(SoC_{swing}, SoC_{avg})$ . We delete the cycle labeled by the shade and update the value of  $D_{SoH,period}$  using:

$$D_{SoH,period} \leftarrow D_{SoH,period} + D_{SoH,cycle}(SoC_{swing}, SoC_{avg}) \quad (7)$$

The updating procedures of  $D_{SoH,period}$  in the other five cases are similar and thus not explained in detail. We continue this procedure until only one cycle, i.e., the cycle with the largest SoC swing, remains in the SoC profile of the battery. Then we obtain an effective estimate value of  $D_{SoH,period}$ . It is provable that charging/discharging cycles with arbitrary patterns can be decoupled using this procedure to a set of charging/discharging cycles with potentially different SoC swings and different average SoC levels. Therefore, we effectively calculate  $D_{SoH,period}$  using this decoupling procedure.

### III. SYSTEM MODEL AND PROBLEM FORMULATION

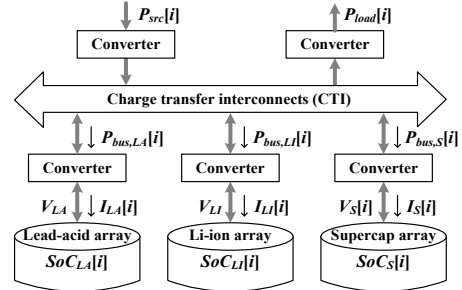


Figure 5: Structure of the HEES system considered in this paper.

Figure 5 presents the HEES system architecture, which consists of a lead-acid battery bank, a Li-ion battery bank, and a supercapacitor bank. Lead-acid batteries are much cheaper than Li-ion batteries, yet they suffer a shorter cycle life and higher power loss during charging and discharging due to more severe rate capacity effect. Supercapacitors are more expensive than both batteries. However, supercapacitors have nearly 100% charging and discharging efficiencies and orders-of-magnitude longer cycle life than batteries.

We use a *slotted time model*, i.e., all the system constraints as well as decisions are provided for discrete time intervals of equal length. More specifically, the whole time period of charge management is divided into  $N$  time slots, each of duration  $\Delta T$ .

Let  $P_{src}[i]$  and  $P_{load}[i]$  ( $1 \leq i \leq N$ ) denote power generation of the power source and power consumption of the electric load, respectively. Let  $SoC_{LA}[i]$ ,  $SoC_{LI}[i]$ , and  $SoC_S[i]$  denote the SoC values of the lead-acid battery array, the Li-ion battery array, and the supercapacitor array, respectively. Let  $V_{LA}$  and  $V_{LI}$  denote the terminal voltages of the lead-acid battery array and the Li-ion battery array, respectively. We neglect the dependency of the battery terminal voltages on the SoC values because the terminal voltages are nearly constant in the major SoC operation range of 20% to 80% [9]. On the other hand, let  $V_S[i]$  denote the terminal voltage of the supercapacitor element array at time slot  $i$ , which is a linear function of SoC. Moreover, the charging/discharging currents of the lead-acid battery array, the Li-ion battery array, and the supercapacitor array are denoted by  $I_{LA}[i]$ ,  $I_{LI}[i]$ , and  $I_S[i]$ , respectively. The current values are positive when charging the EES array and negative when discharging.

The *rate capacity effect* of batteries explains that the charging and discharging efficiencies decrease with the increasing of charging and discharging currents, respectively. More precisely, the Peukert's formula [9] describes that the charging and discharging efficiencies of a battery element array, as functions of the charging current  $I_c$  and discharging current  $I_d$ , respectively, are given by

$$\eta_{rate,c}(I_c) = \frac{k_c}{(I_c)^{\alpha_c}}, \quad \eta_{rate,d}(I_d) = \frac{k_d}{(I_d)^{\alpha_d}} \quad (8)$$

where  $k_c$ ,  $\alpha_c$ ,  $k_d$ , and  $\alpha_d$  are constants. We define equivalent current inside battery array as the actual charge accumulating/reducing speed. We calculate equivalent current  $I_{eq,LA}$  for lead-acid battery array by:

$$I_{eq,LA} = \begin{cases} I_{LA} \cdot \eta_{rate,c,LA}(I_{LA}), & \text{if } I_{LA} > 0, \\ I_{LA}/\eta_{rate,d,LA}(|I_{LA}|), & \text{if } I_{LA} < 0. \end{cases} \quad (9)$$

The equivalent current of the Li-ion battery array can be calculated in the similar way (but less rate capacity effect.) The supercapacitor arrays have negligible rate capacity effect, i.e.,  $I_{eq,S} \approx I_S$ .

For the lead-acid battery array, we calculate  $SoC_{LA}[i]$  from the initial SoC  $SoC_{LA}[1]$  using *Coulomb counting*:

$$SoC_{LA}[i] = SoC_{LA}[1] + \frac{\sum_{j=1}^{i-1} I_{eq,LA}[j] \cdot \Delta T}{C_{full,LA}} \quad (10)$$

where  $C_{full,LA}$  is the full charge capacity of the lead-acid battery array. Similar notations also apply for the Li-ion battery and the supercapacitor by replacing the subscript  $LA$  by  $LI$  and  $S$ , respectively.

The power conversion circuitries exploited in the system consume a significant portion of power. We denote the power conversion efficiencies of various converters at the  $i^{\text{th}}$  time slot by  $\eta_{conv,LA}$ ,  $\eta_{conv,LI}$ ,  $\eta_{conv,S}$ ,  $\eta_{conv,src}$ , and  $\eta_{conv,load}$ . We use  $P_{bus,LA}[i]$ ,  $P_{bus,LI}[i]$ , and  $P_{bus,S}[i]$  ( $1 \leq i \leq N$ ) to denote the power flowing into the lead-acid battery bank, the Li-ion battery bank, and the supercapacitor bank from the CTI, respectively.  $P_{bus,LA}[i]$  satisfies the following equation:

$$P_{bus,LA}[i] = \begin{cases} V_{LA} \cdot I_{LA}[i] / \eta_{conv,LA}, & \text{if } I_{LA}[i] > 0, \\ V_{LA} \cdot I_{LA}[i] \cdot \eta_{conv,LA}, & \text{if } I_{LA}[i] < 0. \end{cases} \quad (11)$$

$P_{bus,LI}[i]$  and  $P_{bus,S}[i]$  also satisfy similar relationships. Moreover, we have the following equation due to the energy conservation law:

$$P_{bus,LA}[i] + P_{bus,LI}[i] + P_{bus,S}[i] = P_{src}[i] \cdot \eta_{conv,src} - \frac{P_{load}[i]}{\eta_{conv,load}} \quad (12)$$

### A. Problem Formulation

The objective of the SoH-aware HEES system control algorithm is to minimize the SoH degradation while satisfying the load power requirements. We define a new objective function, the *overall value degradation*, which captures the different cycle lives and capital cost values of two types of batteries. Let  $D_{SoH,period,LA}$  and  $D_{SoH,period,LI}$  denote the SoH degradation of the lead-acid battery array and Li-ion battery array during charge management, respectively. Let  $D_{SoH,end}$  denote the amount of SoH degradation indicating the end-of-life of a battery array (i.e.,  $D_{SoH,end} = 20\%$ ). The capital cost values of the lead-acid battery array and the Li-ion battery array are given by  $Cost_{LA}$  and  $Cost_{LI}$ , respectively. Then the overall value degradation is

$$Cost_{LA} \cdot \frac{D_{SoH,period,LA}}{D_{SoH,end}} + Cost_{LI} \cdot \frac{D_{SoH,period,LI}}{D_{SoH,end}} \quad (13)$$

The SoH-aware HEES system control problem is described as follows:

**Given:** Power source and load device power profiles  $P_{src}[i]$ ,  $P_{load}[i]$ , respectively, for  $1 \leq i \leq N$ , initial supercapacitor SoC  $SoC_S[1]$ .

**Optimization variables:** Initial SoC's  $SoC_{LA}[1]$  and  $SoC_{LI}[1]$ , EES array charging/discharging currents  $I_{LA}[i]$ ,  $I_{LI}[i]$ ,  $I_S[i]$  for  $1 \leq i \leq N$ .

**Minimize:** the overall value degradation given by Eqn. (13).

**Subject to:**

- i) *Load Power Requirement Constraint:* (12) is satisfied.
- ii) *Capacity and Power Rating Constraints:* Each EES array SoC cannot be less than zero or more than 100%, i.e.,

$$0 \leq SoC_{LA}[i], SoC_{LI}[i], SoC_S[i] \leq 100\% \quad (14)$$

Moreover, the charging/discharging current of each EES array cannot exceed a maximum value, i.e.,

$$-I_{LA,MAX,d} \leq I_{LA}[i] \leq I_{LA,MAX,c} \quad (15)$$

$$-I_{LI,MAX,d} \leq I_{LI}[i] \leq I_{LI,MAX,c} \quad (16)$$

$$-I_{S,MAX,d} \leq I_S[i] \leq I_{S,MAX,c} \quad (17)$$

- iii) *Final Energy Constraints:* EES array SoC at the end of the charge management period should be no less than the initial SoC value:

$$SoC_{LA}[N+1] \geq SoC_{LA}[1], SoC_{LI}[N+1] \geq SoC_{LI}[1], \quad (18)$$

$$SoC_S[N+1] \geq SoC_S[1]$$

## IV. SOH-AWARE CHARGE MANAGEMENT ALGORITHM

We derive a near-optimal SoH-aware charge management policy based on the convex optimization technique. We need to find the near-

optimal values of the initial SoC's  $SoC_{LA}[1]$  and  $SoC_{LI}[1]$ , as well as the EES array current profiles  $I_{LA}[i]$ ,  $I_{LI}[i]$ ,  $I_S[i]$  for  $1 \leq i \leq N$ . The proposed optimization method consists of an outer loop and a kernel algorithm. The outer loop finds near-optimal values of  $SoC_{LA}[1]$  and  $SoC_{LI}[1]$  using ternary search, in order to minimize the overall value degradation while satisfying load power requirement (12). The kernel algorithm finds the optimal EES array current profiles  $I_{LA}[i]$ ,  $I_{LI}[i]$ ,  $I_S[i]$  for  $1 \leq i \leq N$ . The general procedure is shown in Algorithm 1. In the rest of this section, we describe the kernel algorithm in detail.

---

### Algorithm 1: Deriving the SoH-aware charge management policy.

---

**Perform** ternary search to find the optimal  $SoC_{LA}[1]$  and  $SoC_{LI}[1]$ :

*The kernel algorithm:*

Step I: Feasibility check.

Step II: Derive the optimal EES array current profiles  $I_{LA}[i]$ ,  $I_{LI}[i]$ ,  $I_S[i]$  for  $1 \leq i \leq N$  to minimize overall value degradation, given by Eqn. (13).

Find the optimal values of all optimization variables, such that the overall value degradation is minimized and constraints are satisfied.

---

### A. The Kernel Algorithm

The kernel algorithm consists of two steps: Feasibility check and the subsequent optimization of EES array current profiles.

#### 1) Feasibility Check

In this step, we are given  $SoC_{LA}[1]$  and  $SoC_{LI}[1]$  from outer loop. We perform feasibility check, i.e. check whether it is possible to find the EES array current profiles  $I_{LA}[i]$ ,  $I_{LI}[i]$ ,  $I_S[i]$  for  $1 \leq i \leq N$  such that all the constraints (12), (14) – (18) are satisfied. We formulate the feasibility check problem as a convex constraint satisfaction problem (convex CSP) and optimally solve this problem in polynomial time.

First, we define the *energy increasing/decreasing rates* inside the lead-acid battery array, the Li-ion battery array, and the supercapacitor array by  $P_{eq,LA}[i]$ ,  $P_{eq,LI}[i]$ , and  $P_{eq,S}[i]$ , respectively, satisfying:

$$P_{eq,LA}[i] = V_{LA} \cdot I_{eq,LA}[i] \quad (19)$$

$$P_{eq,LI}[i] = V_{LI} \cdot I_{eq,LI}[i] \quad (20)$$

$$P_{eq,S}[i] = V_S[i] \cdot I_{eq,S}[i] = V_S[i] \cdot I_S[i] \quad (21)$$

In the problem formulation, we use  $P_{eq,LA}[i]$ ,  $P_{eq,LI}[i]$ , and  $P_{eq,S}[i]$  ( $1 \leq i \leq N$ ) as the optimization variables instead of the EES array current profiles  $I_{LA}[i]$ ,  $I_{LI}[i]$ ,  $I_S[i]$  ( $1 \leq i \leq N$ ). This will transform the problem into a convex CSP as we shall see in the following. The HEES controller can easily calculate the values of control variables  $I_{LA}[i]$ ,  $I_{LI}[i]$ ,  $I_S[i]$  ( $1 \leq i \leq N$ ) from the derived values of  $P_{eq,LA}[i]$ ,  $P_{eq,LI}[i]$ , and  $P_{eq,S}[i]$  using Eqns. (9), (19) – (21).

We rewrite (12) to make it a convex inequality constraint:

$$P_{bus,LA}[i] + P_{bus,LI}[i] + P_{bus,S}[i] \leq P_{src}[i] \cdot \eta_{conv,src} - \frac{P_{load}[i]}{\eta_{conv,load}} \quad (22)$$

Both the energy conservation law and the load power requirement are still satisfied in (22). We know that  $P_{bus,LA}[i]$ ,  $P_{bus,LI}[i]$ , and  $P_{bus,S}[i]$  are convex functions of  $P_{eq,LA}[i]$ ,  $P_{eq,LI}[i]$ , and  $P_{eq,S}[i]$ , respectively, from Eqns. (9) and (11). This proves that constraint (22) is a convex inequality constraint. Moreover, the other constraints (14) – (18) can be translated into linear inequality constraints of  $P_{eq,LA}[i]$ ,  $P_{eq,LI}[i]$ , and  $P_{eq,S}[i]$  ( $1 \leq i \leq N$ ). Details are omitted due to space limitation.

Then the feasibility check problem becomes a convex CSP [10] because all the constraints are convex inequality constraints. We set the objective function to be a constant value  $Const$  in order to solve this feasibility check problem using standard convex optimization tools. After the feasibility check, we calculate the average SoC levels  $SoC_{avg,LA}$  and  $SoC_{avg,LI}$  from the derived  $P_{eq,LA}[i]$  and  $P_{eq,LI}[i]$  profiles. These average SoC values are important in the subsequent step.

#### 2) Minimizing the Overall Value Degradation

We perform optimization to find the optimal values of  $P_{eq,LA}[i]$ ,  $P_{eq,LI}[i]$ , and  $P_{eq,S}[i]$  ( $1 \leq i \leq N$ ) in order to minimize the overall value degradation given by Eqn. (13). We make use of the following observation in deriving the near-optimal charge management policy:

**Observation III:** Notice that it is possible to decouple the charging and discharging profile of a (lead-acid or Li-ion) battery array into a set of charging/discharging cycles. The cycle with the largest SoC swing has the most significant contribution to the SoH degradation.

Based on Observation III, we focus on minimizing the overall value degradation induced by the charging/discharging cycle (after decoupling) with the largest SoC swing for both battery arrays. Minimizing this objective function helps in minimizing the overall value degradation induced by the other charging/discharging cycles as well. Of course, when calculating the SoH degradation during an operation period, the novel model derived in Section II is used.

For the lead-acid battery array, the largest SoC swing in all the charging/discharging cycles is given by:

$$SoC_{swing,LA}^{MAX} = \max_{1 \leq j \leq N} \left| \frac{\sum_{k=j}^i I_{eq,LA}[k] \cdot \Delta T}{C_{full,LA}} \right| \quad (23)$$

$SoC_{swing,LA}^{MAX}$  is a convex function of  $P_{eq,LA}[i]$  ( $1 \leq i \leq N$ ) because pointwise maximum of a set of convex function is still convex [10]. Similarly, we calculate the largest SoC swing  $SoC_{swing,LI}^{MAX}$  for Li-ion battery array. Moreover, let  $D_{SoH,cycle,LA}(SoC_{swing}, SoC_{avg})$  denote the SoH degradation of lead-acid array in one charging/discharging cycle as a function of SoC swing  $SoC_{swing}$  and average SoC  $SoC_{avg}$ . Similarly, we define the function  $D_{SoH,cycle,LI}(SoC_{swing}, SoC_{avg})$  for the Li-ion battery array. We minimize the overall value degradation contributed by the charging/discharging cycles with largest SoC swing for both battery arrays. The objective is given by:

$$Cost_{LA} \cdot \frac{D_{SoH,cycle,LA}(SoC_{swing,LA}^{MAX}, SoC_{avg,LA})}{D_{SoH,end}} + Cost_{LI} \cdot \frac{D_{SoH,cycle,LI}(SoC_{swing,LI}^{MAX}, SoC_{avg,LI})}{D_{SoH,end}} \quad (24)$$

where we use average SoC levels obtained from the feasibility check as estimation of average SoC levels  $SoC_{avg,LA}$  and  $SoC_{avg,LI}$  in (24). Objective function (24) is a convex function of  $P_{eq,LA}[i]$  and  $P_{eq,LI}[i]$  ( $1 \leq i \leq N$ ) because: (i)  $D_{SoH,cycle,LA}(SoC_{swing}, SoC_{avg})$  and  $D_{SoH,cycle,LI}(SoC_{swing}, SoC_{avg})$  are convex and monotonically increasing functions of  $SoC_{swing}$  when  $SoC_{avg}$  is given, and (ii)  $SoC_{swing,LA}^{MAX}$  and  $SoC_{swing,LI}^{MAX}$  are convex functions of  $P_{eq,LA}[i]$  and  $P_{eq,LI}[i]$  ( $1 \leq i \leq N$ ), respectively, as mentioned before.

The constraints of this optimization problem are the same as those in the feasibility check problem. Therefore, the overall value degradation minimization described in this part is a convex optimization problem because it has convex objective function and convex inequality constraints. We find the optimal solution in polynomial time.

## V. SIMULATION RESULTS

We derive and implement the proposed SoH-aware charge management policy on a typical HEES system comprised of a lead-acid battery bank, a Li-ion battery bank, and a supercapacitor bank. The lead-acid battery bank has 3 Ah nominal capacity and 20 V terminal voltage. The Li-ion battery bank has 4 Ah nominal capacity and 15 V terminal voltage. The supercapacitor bank has 200 F capacitance.

We compare the cycle life of the proposed system with two baseline systems. Baseline 1 uses a HEES system comprised of a lead-acid battery bank and a Li-ion battery bank that are the same as the proposed system, but without the supercapacitor bank. Baseline 2 uses the same HEES system as the proposed system. Both baseline systems exploit the optimal HEES control policy in order to satisfy the load power requirement and improve the HEES system cycle efficiency. The load power requirement is satisfied in all systems.

We perform experiments based on synthesized source and load power profiles as shown in Figure 6. We compare the SoH degradation and cycle life of both battery arrays between the proposed system and two baseline systems, with results shown in Table I. The proposed system achieves significantly smaller SoH degradation rate, and hence, larger cycle life, compared with both baseline systems. It achieves a cycle life improvement up to 17.3X compared with Baseline 1 thanks

to the contributions of both the supercapacitor bank and the SoH-aware control policy. The maximum cycle life improvement compared with Baseline 2 is 3.5X due to the SoH-aware control policy solely.

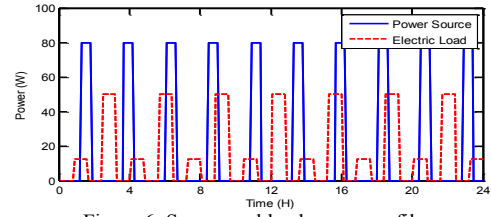


Figure 6: Source and load power profiles.

Table I. SoH degradation and cycle life comparison between the proposed system and baseline systems using synthesized power profiles.

		Compare with Baseline 1	Compare with Baseline 2
Lead-acid	SoH degradation	10.6%	33.2%
	Cycle life	9.4X	3.0X
Li-ion	SoH degradation	5.8%	28.7%
	Cycle life	17.3X	3.5X

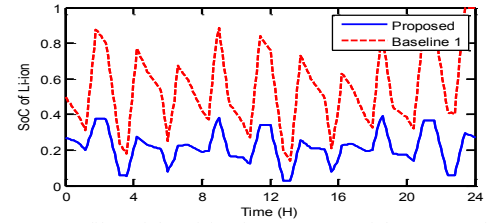


Figure 7: SoC profiles of the Li-ion battery array of the proposed system and Baseline 1 under synthesized power profiles.

We provide the SoC profile versus time for the proposed system and Baseline 1 as shown in Figure 7. The maximum SoC swing and average SoC level of the Li-ion battery array have been reduced by 35% and 30%, respectively. The former accounts for about 6X improvement in cycle life whereas the latter accounts for about 3X.

## VI. CONCLUSION

Cycle life of EES elements is one of the most important metrics that should be considered. Cycle life is related to SoH degradation. SoH degradation models presented in the reference papers can only be applied in the cases of constant-current cycled charging and discharging with the same SoC swing in each cycle. This work is the first attempt to derive a novel SoH degradation model that estimates SoH degradation rate under arbitrary charging and discharging patterns of a battery. We also introduce a near-optimal charge management policy based on the proposed SoH degradation model focusing on extending cycle life of the batteries in the HEES systems while simultaneously improving the overall cycle efficiency.

## REFERENCES

- [1] J. Baker and A. Collinson, "Electrical energy storage at the turn of the millennium," *Power Engineering Journal*, 1999.
- [2] M. Pedram, N. Chang, Y. Kim, and Y. Wang, "Hybrid electrical energy storage systems," in *ISLPED*, 2010.
- [3] F. Koushanfar, "Hierarchical hybrid power supply networks," in *Design Automation Conference (DAC)*, 2010.
- [4] Y. Wang, Y. Kim, Q. Xie, N. Chang, and M. Pedram, "Charge migration efficiency optimization in hybrid electrical energy storage (HEES) systems," in *ISLPED*, 2011.
- [5] Q. Xie, Y. Wang, Y. Kim, N. Chang, and M. Pedram, "Charge allocation for hybrid electrical energy storage systems," in *CODES+ISSS*, 2011.
- [6] A. Millner, "Modeling Lithium Ion battery degradation in electric vehicles," *IEEE CITRES*, 2010.
- [7] M. Dubbary et al., "Capacity and power fading mechanism identification from a commercial cell evaluation," *Journal of Power Sources*, 2007.
- [8] Q. Xie, X. Lin, Y. Wang, M. Pedram, D. Shin, and N. Chang, "State of health aware charge management in hybrid electrical energy storage systems," in *Design, Automation, and Test in Europe (DATE)*, 2012.
- [9] D. Linden and T. B. Reddy, *Handbook of Batteries*, McGraw-Hill Professional, 2001.
- [10] S. Boyd and L. Vandenberghe, *Convex Optimization*, Cambridge University Press, 2004.